Macromolecules

Article

pubs.acs.org/Macromolecules

3,6-Carbazole Incorporated into Poly[9,9-dioctylfluorene-*alt*-(bisthienyl)benzothiadiazole]s Improving the Power Conversion Efficiency

Yuanhe Fu,[†] Hyojung Cha,[†] Gang-Young Lee, Byung Joon Moon, Chan Eon Park, and Taiho Park*

Department of Chemical Engineering, Pohang University of Science and Technology, San31, Nam-gu, Pohang, Gyeongbuk, 790-780, Korea

Supporting Information

ABSTRACT: A novel concept of D−A-type copolymers based on fluorene polymer incorporated with 3,6-carbazole unit enhances the device performance for organic photovoltaic cells. **P($F_{45}C_5$-DTBT)**, incorporating 5 mol % 3,6-carbazole into **P(2,7F-DTBT)**, shows an almost 2-fold improvement (5.1%) in power conversion efficiency relative to **P(2,7F-DTBT)** (2.6%). This results is ascribed to the good balance between electron and hole mobilities in the devices ($\mu_e/\mu_h \sim 1.8$ for **P($F_{45}C_5$-DTBT)** vs 152 for **P(2,7F-DTBT)**), and the formation of a nanoscale morphology in the blend of the copolymer and [6,6]-phenyl C71-butyric acid methyl ester ($PC_{71}BM$).

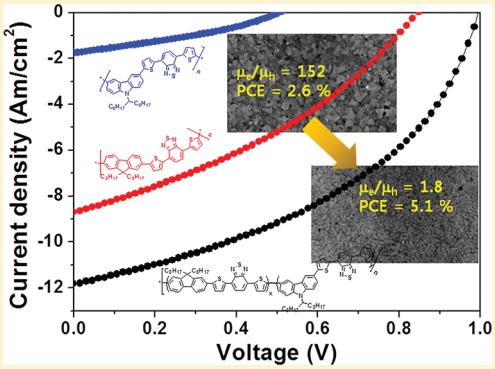

INTRODUCTION

Organic photovoltaic solar cells (OPVs) have been under development for a couple of decades in an effort to capitalize on their low cost, flexibility, tunability with respect to light-harvesting capabilities, lightweight properties, and large-area processability.[1] OPVs could be fabricated from a blend of photoactive conducting polymers and fullerene derivatives, forming bulk heterojunctions.[1,2] Much effort has been applied toward developing a variety of photoactive conducting polymers.[3] Among such polymers, electron donor− (D−) electron acceptor (A) type copolymers show promise and are widely used for harvesting solar energy over a broad spectral range.[4] For instance, poly[4,4-bis(2-ethylhexyl)dithieno(3,2-*b*:2′,3′-*d*)silole-*alt*-*N*-octylthieno(3,4-*c*)pyrrole-4,6-dione],[3a] poly[benzo(1,2-*b*:4,5-*b*′)dithiophene-*alt*-5,6-difluoro-4,7-di-thien-2-yl-2,1,3-benzothiadiazole (PBnDTDTffBT),[3b] poly[4,8-bis-substituted-benzo(1,2-*b*:4,5-*b*′)dithiophene-2,6-diyl-*alt*-4-substituted-thieno(3,4-b)thiophene-2,6-diyl] (PBDTTT),[5] and its fluorinated polymer (PBDTTT-CF)[5] exhibited power conversion efficiencies (PCEs) in the range 7.2−7.7%. An important consideration for developing novel copolymers is cost. With that in mind, easy large-scale synthetic approaches that rely on low-cost materials provide the most attractive commercial opportunities and are, therefore, in high demand.

Dioctylfluorene 2,7-diborate (**1**) is an easily scalable fused-aromatic monomer and has been widely investigated for use in organic light emitting diodes (OLEDs) and organic field effect transistors (OFETs).[6] D−A copolymers employing 2,7-fluorene, poly[9′,9′-dioctyl-2,7-fluorene-*alt*-5,5-(4′,7′-di-2-thien-yl-2′,1′,3′-benzothiadiazole)] (**P(2,7F-DTBT)**) have been used in OPVs, yielding PCEs of 0.75%, which can be improved up to 2.84% by optimizing the film morphology.[7] The short-circuit current density (J_{SC}) can be influenced by several parameters, including the molecular weight of the copolymer, overlap between the absorption spectrum and the solar illumination spectrum, the exciton dissociation rate, the film morphology, and the charge carrier mobility. More importantly, the hole ($\mu_{h,blend}$) and electron ($\mu_{e,blend}$) mobilities in a blend should be well balanced to promote the continuous generation of electrons without recombination reactions or saturation of charges.[8] Apart from the device structures and fabrication processes, an intrinsic limitation of **P(2,7F-DTBT)** is its low hole mobility, 2.7×10^{-6} $cm^2 V^{-1} s^{-1}$, measured using the space charge limited current (SCLC) method[9] (see Table 1). One method for improving Jsc is to increase the hole mobility ($\mu_{h,polymer}$) of **P(2,7F-DTBT)**, leading to a good balance between $\mu_{e,blend}$ and $\mu_{h,blend}$ in a device (e.g., $\mu_e/\mu_h \sim 1$).

Recently, we reported the synthesis of a series of copolymers **P(F_xC_y-DTBT)** prepared from a Suzuki condensation polymerization of fluorene 2,7-diborate, carbazole 3,6-diborate and bis(bromothienyl)benzothiadiazole as shown in Figure 1a. The copolymers included conjugation breaks to the 3,6-linkages in the resulting polymers.[10] As a result, the polymers showed a highly coplanar structure that formed strong intramolecular charge complexes with strong $\pi-\pi$ stacking between conjugation breaks. Thus, inclusion of conjugation breaks in

Received: February 3, 2012
Revised: March 8, 2012
Published: March 23, 2012

   dx.doi.org/10.1021/ma3002438 | *Macromolecules* 2012, 45, 3004−3009

Table 1. Summary of GPC, Spectroscopic, and Hole Mobility Data for the Copolymers[a]

device	$M_n/10^3$ (g/mol)[b]	Tg (°C)[c]	ε_{abs} (dm^3 mol^{-1}cm^{-1})[d]	λ_{max} (nm)[e]	E_{opt} (eV)[f]	HOMO (eV)[g]	$\mu_h/10^{-6}$ (cm^2/(V s))[h]
P(2,7F-DTBT)	18.4(2.2)	113	38 000	564	1.92	−5.50	2.7
P($F_{49}C_1$-DTBT)	11.4(3.8)	119	37 800	558	1.89	−5.56	3.5
P($F_{45}C_5$-DTBT)	14.5(2.9)	120	37 000	549	1.88	−5.51	4.1
P($F_{40}C_{10}$-DTBT)	8.3(1.5)	122	33 300	559	1.88	−5.50	4.3
P(3,6C-DTBT)	4.1(1.1)	161	22 000	551	1.85	−5.18	12.0

[a]Data for the two control polymers [**P(2,7F-DTBT)** and **P(3,6C-DTBT)**], and **P($F_{45}C_5$-DTBT)** were taken from our previous reports[10,11] and **P($F_{49}C_1$-DTBT)** and **P($F_{40}C_{10}$-DTBT)** were synthesized and characterized in this work (see Figures S1 and S2, Supporting Information, for the DSC thermograms and cyclic voltamograms). [b]Number-average molecular weight determined by GPC in chloroform using polystyrene standards. The polydispersity index (M_w/M_n) is given in parentheses. [d]Absorption coefficient measured in a $CHCl_3$ solution (dm^3 mol^{-1}cm^{-1}). [c]DSC curves were in the Supporting Information (Figure S1). [e]Absorption maxima from the intramolecular charge complexes in the film state. [f]Optical band gap in a film. [g]Estimated in the film state (Figure S2, Supporting Information). [h]Extracted and calculated from space charge limited current (SCLC) measurements in hole-only devices.

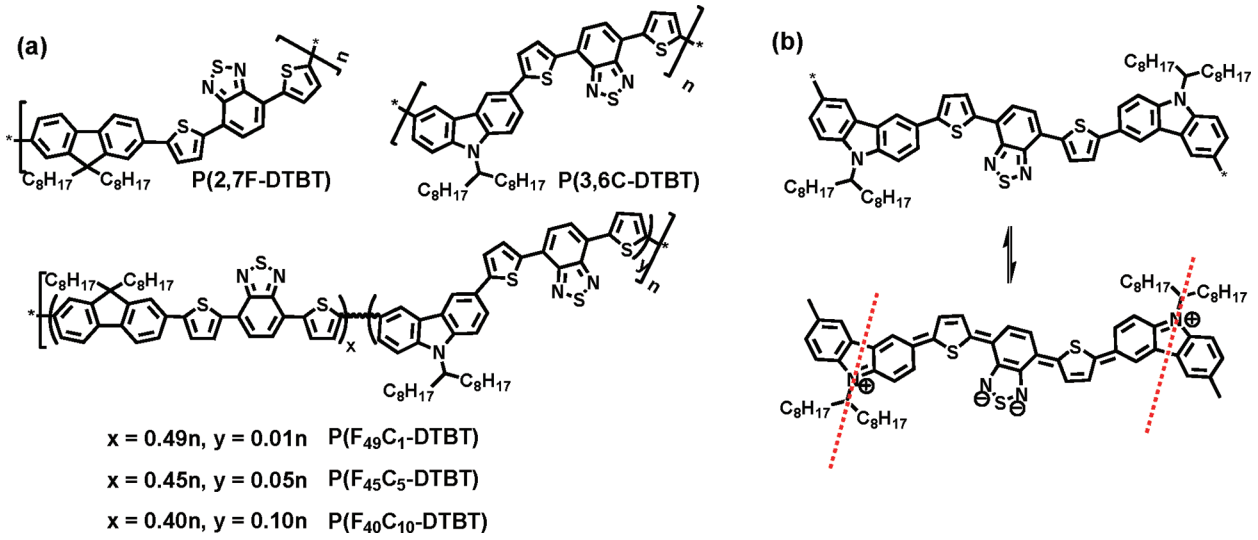

Figure 1. (a) Chemical structures of **P(2,7F-DTBT)**, **P(3,6C-DTBT)**, **P($F_{49}C_1$-DTBT)**, **P($F_{45}C_5$-DTBT)**, and **P($F_{40}C_{10}$-DTBT)**. (b) Equilibria between the aromatic structure and the quinoid structure in **P(3,6C-DTBT)**. The dotted line indicates a conjugation break.

the **P(2,7F-DTBT)** structure improved the hole mobility and $\pi-\pi$ stacking between copolymer chains.[11]

Herein, we report a novel concept to enhance the photovoltaic performance of D−A-type copolymers prepared from easily scalable fused-aromatic monomers (e.g., octylfluorene 2,7-diborate). **P(F_xC_y-DTBT)**, incorporating y mol % 3,6-carbazole into **P(2,7F-DTBT)**, shows a great improvement in PCE relative to **P(2,7F-DTBT)**, due to the good balance between electron and hole mobilities in the devices (e.g., $\mu_e/\mu_h \sim 1.8$ for **P($F_{45}C_5$-DTBT)** and **P($F_{45}C_5$-DTBT)**, vs 152 for **P(2,7F-DTBT)**) and the formation of a nanoscale morphology in the blend of the copolymer and [6,6]-phenyl C71-butyric acid methyl ester ($PC_{71}BM$).

The balance between carrier generation by extraction and carrier losses by recombination leads to a distinct optimum in the carrier mobility with regard to the efficiency of organic solar cells.[12] We have shown that the maximum performance of organic solar cells is governed by the balance between transport and recombination of charge carriers through incorporating a small amount of 3,6-carbazole moiety into **P(2,7F-DTBT)**.

EXPERIMENTAL SECTION

Materials. All chemicals were purchased from Sigma-Aldrich Co, Junsei Co and used without further purification. 2,7-Bis(4′,4′,5′,5′-tetramethyl-1′,3′,2′-dioxaborolan-2′-yl)-9,9-dioctylfluorene and 4,7-bis-(5-bromo-2-thienyl)-2,1,3-benzothiadiazole (**DTBT**) were prepared according to the literature.[13] 3,6-bis(4′,4′,5′,5′-tetramethyl-1′3′2′-dioxaborolan-2′-yl)-*N*-9″-heptadecanylcarbazole was synthesized following the same procedure as we previously reported.[2] Preparation of **P(2,7F-DTBT)**, **P(3,6C-DTBT)**, **P($F_{45}C_5$-DTBT)** were described in our previous reports.[10,11]

Instrumentation. Microwave irradiation experiments were performed using "Monowave 300" single-mode microwave reactor with a maximum of 850 W magnetron output power. ^{1}H and ^{13}C NMR spectra were recorded on a Bruker BioSpin AG system operated at 400 MHz using tetramethylsilane (TMS; $\delta = 0$) as internal standard. Number−average (M_n) and weight-average (M_w) molecular weights were determined by gel permeation chromatography (GPC) using the Shimadzu LC solution, chloroform as the eluent with a flow rate of 1.0 mL/min, and polystyrenes as standards to calibrate. UV−vis absorption and photoluminescence spectra were obtained using a Carry 5000 UV−vis−near-IR double beam spectrophotometer and FR 650, JASCO spectrophotometer, respectively. Cyclic voltammetry (CV) was performed using a PowerLab/AD instrument model system in 0.1 M solution of tetrabutylammonium hexafluorophospate (Bu_4NPF_6) in anhydrous acetonitrile as supporting electrolyte at a scan rate of 50 mV s^{-1}. A glassy carbon disk (~0.05 cm^2) coated with a thin polymer film, an $Ag/AgNO_3$ electrode, and a platinum wire were used as working electrode, reference electrode, and counter electrode, respectively. Differential scanning calorimetric (DSC) measurements of the copolymers were performed using a Seiko DSC 220 CU instrument under a nitrogen atmosphere at a heating cooling rate of 10 °C/min. The atomic force microscope (AFM) (Multimode IIIa, Digital Instruments) was operated in tapping mode to acquire images of the surfaces of polymers films. Films were prepared by dissolving

dx.doi.org/10.1021/ma3002438 | *Macromolecules* 2012, 45, 3004−3009

the copolymer and $PC_{71}BM$ in dichlorobenzene, followed by spin-coating on the top surface of a PEDOT:PSS substrate. The prepared samples were annealed at 120 °C on a hot plate under nitrogen. TEM images were obtained using a HITACHI-7600 operated at 100 kV. The polymers:$PC_{71}BM$ layers were floated from the water-soluble PEDOT:PSS substrate onto the surface of dematerialized water and picked up with 200-mesh copper TEM grids.

Synthesis of P($F_{40}C_{10}$-DTBT). To a microwave reactor vial containing 9-dioctylfluorene-diboronate (180 mg, 0.28 mmol), the 3,6-carbazole diboronate (21 mg, 0.031 mmol) and DTBT (143 mg, 0.31 mmol) in a mixture of degassed toluene (3 mL) and Et_4NOH 20% solution in water (1 mL) was added a catalyst of tetrakis-(triphenylphosphine)palladium(0) (5 mg) and three drops of Aliquat 336. The mixture was allowed to stir for 2 h at 110 °C. After reaction completion and cooling to room temperature, the mixture was poured into methanol (200 mL). The precipitated solid was recovered by filtration in a Soxhlet thimble and extracted with acetone, hexane and chloroform for 24 h each. To the chloroform fraction was added ethylenediaminetetraacetate (EDTA) (150 mg, 0.403 mmol) and stirred for 6 h. Then the organic fraction was washed with demineralized water (200 mL) three times and concentrated under reduced pressure. The residue was precipitated in a vigorously stirred methanol (200 mL) and the desired dark violet polymers were obtained: (130 mg, 61%). M_n = 8300, M_w = 12 800, PDI = 1.54. ^{1}H NMR (400 MHz, $CDCl_3$, ppm): δ 8.16−6.99 (m, 12H); 2.01 (br, 2H); 1.52 (br, 2H); 1.25 (br, 12H); 0.80 (br, 6H).

Synthesis of P($F_{49}C_1$-DTBT). Following the method for the synthesis of **P($F_{40}C_{10}$-DTBT)** procedure, 198 mg (0.31 mmol) of 9-dioctylfluorene-diboronate, 2 mg (0.003 mmol) of 3,6-carbazole diboronate and 143 mg (0.31 mmol) of DTBT afforded the title copolymer as a dark violet solid (130 mg, 61%). M_n = 11 400, M_w = 42 900, PDI = 3.76. ^{1}H NMR (400 MHz, $CDCl_3$, ppm): δ 8.14−7.25 (m, 12H); 2.05 (br, 3H); 1.53 (br, 2H); 1.09 (br, 20H); 0.78 (br, 9H).

Mobility Measurement. Hole-only devices of the polymers were fabricated on top of a prepatterned ITO substrate. After cleaning the ITO with aqueous detergent, deionized water, acetone, and 2-propanol, UV-ozone treatment was applied for 15 min. PEDOT:PSS (Baytron P TP AI 4083, Bayer AG) was spin-coated from an aqueous dispersion phase to a layer 36 nm thick. The coated substrate was then baked at 120 °C for 60 min. After baking, a solution of the copolymer in chloroform was spin-cast on top of the PEDOT:PSS layer to a thickness of ∼50 nm, and the samples were dried for 6 h at room temperature under vacuum conditions. The Pd electrode was deposited by thermal evaporation under a vacuum of ∼10^{-6} Torr. A similar way was employed to measure the hole only mobility of the polymer:$PC_{71}BM$ blend through the space charge-limited current (SCLC) method with a device structure of ITO/PEDOT:PSS/polymer:$PC_{71}BM$/Au. We also fabricated electron-only devices (Al/copolymer:PCBM/Al) and investigated their $J-V$ characteristics in the dark. The SCLC mobilities were estimated using the Mott−Gurney square law.[14]

$$J = \frac{9}{8}\varepsilon_0\varepsilon_r\mu_h\frac{V^2}{L^3}$$

where J is the current density, L is the film thickness of active layer, μ_h is the hole mobility, ε_r is the relative dielectric constant of the transport medium, ε_0 is the permittivity of free space (8.85×10^{-12} Fm^{1-}), V is the internal voltage in the device and $V = V_{appl} - V_r - V_{bi}$, where V_{appl} is the applied voltage to the device, V_r is the voltage drop due to contact resistance and series resistance across the electrodes, and V_{bi} is the built-in voltage due to the relative work function difference of the two electrodes. The V_{bi} can be determined from the transition between the ohmic region and the SCLC region.

Devices Fabrication and Evaluation. The polymer solar cells were fabricated as following: ITO-coated glass substrates were cleaned with detergent, D.I. water, acetone, and isopropyl alcohol. A thin layer (ca. 40 nm) of PEDOT:PSS (Baytron P VP AI 4083) was first spin-coated on the precleaned ITO-coated glass substrates at 4000 rpm and baked at 120 °C for an hour under ambient conditions. The substrates were then transferred into a nitrogen-filled glovebox. Subsequently, the copolymer:$PC_{71}BM$ active layer (ca. 120 nm) was spin-coated on the PEDOT:PSS layer from a homogeneously blended solution. The solution was prepared by dissolving the polymer at various blend weight ratios of 1:1−1:5 in 1,2-dichlorobenzene and filtered with a 0.2 μm PTFE filter. At the final stage, the substrates were pumped down to high vacuum, and LiF (1 nm) topped with aluminum (100 nm) was thermally evaporated onto the active layer through shadow masks to define the active area of the devices. The thickness of films was measured with a Tencor Alpha-Step 500 profilometer. The unencapsulated solar cells were tested under ambient conditions using a Keithley 2400 SMU and an Oriel xenon lamp (450 W) with an AM1.5 filter. A mask was used to define the device illumination area of 0.06 cm^2 to minimize photocurrent generation from the edge of the electrodes. The solar cells (with no protective encapsulation) were then tested in air under AM 1.5G illumination of 100 mW/cm^2 (Oriel 1 kW solar simulator), which was calibrated with a KG5 filter covered silicon photovoltaic solar cell traceable to the National Renewable Energy Laboratory (NREL). The external quantum efficiency (EQE) was performed using a photomodulation spectroscopic setup (model Merlin, Oriel), a calibrated Si UV detector, and an SR570 low noise current amplifier.

RESULTS AND DISCUSSION

The preparation of the two control polymers [**P(2,7F-DTBT)** and **P(3,6C-DTBT)**] and **P($F_{45}C_5$-DTBT)** were described elsewhere[10,11] and **P($F_{49}C_1$-DTBT)** and **P($F_{40}C_{10}$-DTBT)** were synthesized following the literature.[11] The characterization data are summarized in Table 1 (see Figures S1 and S2, Supporting Information, for DSC thermograms and cyclic voltammograms of the polymers, respectively). The hole mobilities of the copolymers were extracted and calculated from space charge limited current (SCLC) measurements in hole-only devices.[9] The dark current characteristics of the device (ITO/PEDOT:PSS (36 nm)/copolymer (50 nm)/Pd) clearly exhibited ohmic behavior at low voltages and trap-free SCLC behavior at high voltages (see Figure S3, Supporting Information). The hole mobilities of the copolymers series **P(F_xC_y-DTBT)** were improved through increasing the content of 3,6-carbazole unit (y). For instance, **P($F_{49}C_1$-DTBT)**, **P($F_{45}C_5$-DTBT)** and **P($F_{40}C_{10}$-DTBT)** exhibited 3.5×10^{-6}, 4.1×10^{-6} and 4.3×10^{-6} $cm^2/(V\ s)$ of the hole mobility, respectively, smaller than that of **P(3,6C-DTBT)** (1.2×10^{-5} $cm^2/(V\ s)$) but greater than that of **P(2,7F-DTBT)** (2.7×10^{-6} $cm^2/(V\ s)$), even though 1−5 mol % of 3,6-carbazole were incorporated into the main backbone of **P(2,7F-DTBT)**. These results indicated that charges were stabilized by delocalization within the conjugation breaks (Figure 1b),[15] and they were intermolecularly transferred to adjacent hopping sites.

In the preliminary investigation, an optimized weight ratio of a blend of **P($F_{45}C_5$-DTBT)** and $PC_{71}BM$ in o-dichlorobenzene (DCB) was found to be 1:4 with a general structure of ITO/PEDOT:PSS (40 nm)/copolymer:$PC_{71}BM$ (120 nm)/LiF/Al (see Figure S4 and Table S1, Supporting Information). In this condition, we investigated the effect of 3,6-carbazole incorporated into the main backbone of **P(2,7F-DTBT)** on the photovoltaic performance (Figure 2). The $J-V$ characteristics of the devices under AM1.5G (100 mW/cm^2) illumination are summarized in Table 2. An optimized **P(2,7F-DTBT)** device after annealing at 120 °C for 15 min provided a V_{OC} of 0.85 V, a J_{SC} of 8.7 mA/cm^2, and a fill factor (FF) of 0.35, resulting in an estimated PCE of 2.6%, consistent with literature.[9] Meanwhile, the device prepared from **P(3,6C-DTBT)** did not yield photovoltaic properties, even when fabricated under identical conditions, probably due to the low molecular weight

dx.doi.org/10.1021/ma3002438 | Macromolecules 2012, 45, 3004−3009

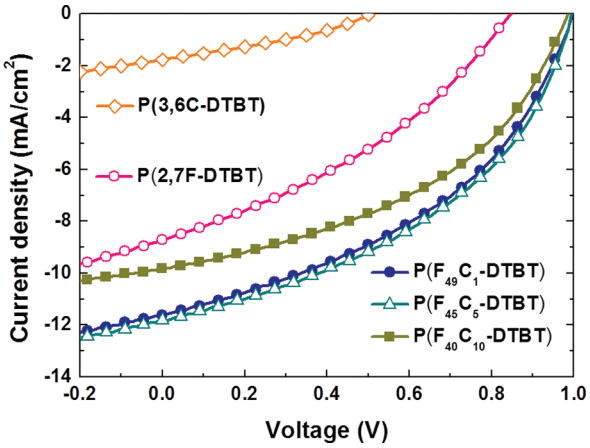

Figure 2. *J*–*V* characteristics for the devices of the blends composed of copolymer:$PC_{71}BM$ (1:4).

Table 2. Photovoltaic Properties of the Copolymer Solar Cells[a]

polymer	V_{OC} [V]	J_{SC} [mA/cm^2]	FF [%]	PCE [%]
P(2,7F-DTBT)	0.85	8.7	35.4	2.6
P($F_{49}C_1$-DTBT)	1.0	11.6	42.4	4.9
P($F_{45}C_5$-DTBT)	1.00	11.8	43.1	5.1
P($F_{40}C_{10}$-DTBT)	0.98	9.8	44.3	4.3
P(3,6C-DTBT)	0.50	1.75	23.6	0.21

[a]A mask was used to define a device illumination area of 0.06 cm^2 to minimize photocurrent generation from the edge of the electrodes. Cell size: 0.06 cm^2 under a mask. Thermal treatment at 120 °C for 15 min. Light intensity: 100 mW/cm^2.

and full conjugation breaks, which shortened the effective conjugation length.[10] On the other hand, incorporation of 3,6-carbazoles into the main backbone of **P(2,7F-DTBT)** greatly improved photovoltaic performance of the devices (2.6% → 4.3–5.1% PCE). The best performance of the device was obtained from **P($F_{45}C_5$-DTBT)** with V_{OC} = 1.00 V, J_{SC} =11.8 mA/cm^2, FF = 0.43, and PCE = 5.1%. The FF (0.43) of the device remained low due to the low hole mobility (4.1×10^{-6} cm^2/(V s))[4b] of the copolymer even though this value was higher than that (FF = 0.35) observed in **P(2,7F-DTBT)**. The V_{OC}s for the optimized devices employing **P(2,7F-DTBT)** and **P($F_{45}C_5$-DTBT)** were 0.85 and 1.00 V, respectively. These values were, respectively, 0.29 and 0.15 V smaller than those estimated from the energy gap (ΔE_{gap} = 1.14 V) between the $LUMO_{PCBM}$ and $HOMO_{copolymer}$.[7] This result indicated that recombination reactions between the photoinduced electrons[8c] and holes were more dominant in **P(2,7F-DTBT)** than in **P($F_{45}C_5$-DTBT)**. Thermal treatment effect was only observed on the copolymers having 3,6-carbazole moiety (see Figure S5 and Table S2, Supporting Information). Device performances employing **P(2,7F-DTBT)** before and after thermal treatments (120 °C for 15 min) were relatively unchanged. In contrast, **P($F_{45}C_5$-DTBT)** exhibited a V_{OC} of 0.98 V, a J_{SC} of 10.8 mA/cm^2, a FF of 0.38, and a PCE of 4.1% prior to thermal treatment. By annealing the device, J_{SC}, FF, and PCE were particularly improved to 11.8 mA/cm^2, 0.43, and 5.1%, respectively (see Figure S6, Supporting Information).

The external quantum efficiency (EQE) and the enhanced EQE spectra for the devices are shown in Figure 3, corresponded to an excellent photocurrent response over the absorption range, covering 300–700 nm. The shapes of the

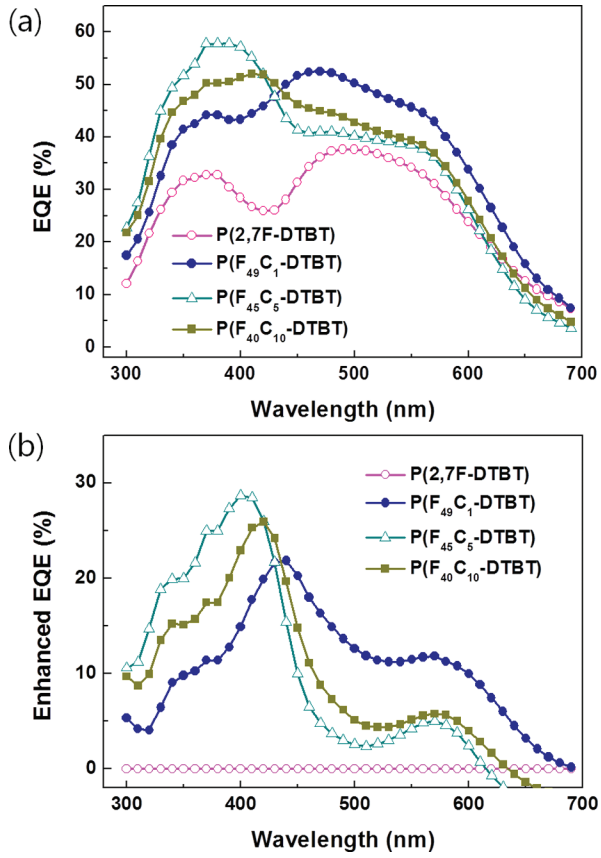

Figure 3. External quantum efficiency (EQE) (a) and enhanced EQE (b) for the devices of the blends composed of copolymer:$PC_{71}BM$ (1:4).

EQE plots for the copolymers are similar to the corresponding absorption spectra (Figure S7, Supporting Information), indicating that all absorption wavelengths of the copolymers contribute to photocurrent generation.

The EQE of the device prepared from **P($F_{49}C_1$-DTBT)** showed a similar shape to **P(2,7F-DTBT)**, but a remarkably enhanced EQE over the absorption range of 300–700 nm was observed (also see Figure S5). The highest EQE value for **P($F_{49}C_1$-DTBT)** approached ca. 54% at 450–500 nm, which was ca. 18% greater than that for **P(2,7F-DTBT)**, despite the slightly lower absorption coefficient in **P($F_{49}C_1$-DTBT)**. For the devices prepared from **P($F_{45}C_5$-DTBT)** and **P($F_{40}C_{10}$-DTBT)**, EQEs were also enhanced, especially in the range of 330–450 nm, probably due to the relatively high content (5–10 mol %) of 3,6-carbazole. 3,6-Carbazole moiety induces conjugation break and reduces the conjugation length in the main backbone of the polymer as we reported previously.[10,16a] These results clearly showed that the enhanced EQEs for **P(F_xC_y-DTBT)s** were consistent with the improved PCEs in the devices.

The maximum J_{SC} of organic BHJ solar cells is governed by the balance between transport and recombination of charge carriers. Imbalanced mobilities of hole and electron could contribute to the large recombination which resulted in a lower J_{SC}.

$$V_{OC} \approx \frac{nkT}{q} \ln\left(\frac{J_{SC}}{J_S}\right)$$

dx.doi.org/10.1021/ma3002438 | *Macromolecules* 2012, 45, 3004–3009

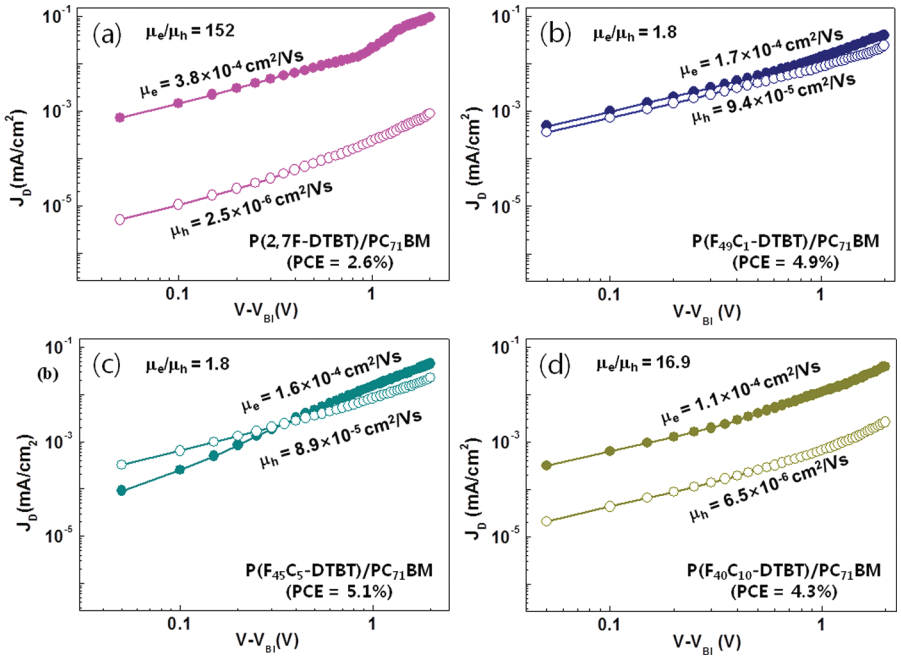

Figure 4. Ratios of electron ($\mu_{e,blend}$, filled circles) and hole ($\mu_{h,blend}$, open circles) mobilities of the blends composed of copolymer:$PC_{71}BM$ (1:4). (a) **P(2,7F-DTBT)**, (b) **P($F_{49}C_1$-DTBT)**, (c) **P($F_{45}C_5$-DTBT)**, and (d) **P($F_{40}C_{10}$-DTBT)**.

Here, n is the diode ideality factor, k is the Boltzmann constant, T is the Kelvin temperature, q is the fundamental charge, J_S is the saturation current density.[16b,c] This equation describes the relationship between V_{OC} and J_{SC}. Therefore, the optimized balance between hole and electron is a key factor for the not only high J_{SC} but also V_{OC}.

We investigated the basis for the improved PCE upon incorporation of 3,6-carbazole. We considered that the imbalance between $\mu_{e,blend}$ and $\mu_{h,blend}$ could contribute to the discrepancy between V_{OC} and $V_{OC,calc}$ due to recombination reactions in the device fabricated with **P(2,7F-DTBT)**, as well as to the greatly improved J_{SC} in the devices fabricated with **P(F_xC_y-DTBT)**s.[8,12]

If the space charges remained in the bulk heterojunction due to a low charge mobility or an imbalance between $\mu_{e,blend}$ and $\mu_{h,blend}$, the photoinduced charge carriers would not be fully extracted and, therefore, would not produce an efficient current under an applied voltage. In this case, the possibility for recombination between holes and electrons at the donor/acceptor interface may increase and J_{SC} and FF may be reduced.

Indeed, large differences were observed between the mobility ratios (μ_e/μ_h) for blends of **P(2,7F-DTBT)**:$PC_{71}BM$, **P($F_{49}C_1$-DTBT)**:$PC_{71}BM$, **P($F_{45}C_5$-DTBT)**:$PC_{71}BM$ and **P($F_{40}C_{10}$-DTBT)**:$PC_{71}BM$ (Figure 4) and the μ_e/μ_hs have a strong relationship with PCEs as seen Figure 4. $\mu_{e,blend}$ and $\mu_{h,blend}$ for a blend of **P(2,7F-DTBT)**:$PC_{71}BM$, calculated using the SCLC model under dark current conditions, were 3.8 × 10^{-4} and 2.5 × 10^{-6} cm^2 V^{-1} s^{-1}, respectively, yielding μ_e/μ_h = 152 (Figure 4(a)). In contrast, μ_e/μ_hs for **P($F_{49}C_1$-DTBT)**:$PC_{71}BM$, **P($F_{45}C_5$-DTBT)**:$PC_{71}BM$ and **P($F_{40}C_{10}$-DTBT)**:$PC_{71}BM$ were 1.8, 1.8, and 16.9, respectively (Figure 4). This result was mainly ascribed to an increase in μ_h (e.g., $\mu_{h,polymer}$ = 4.5 × 10^{-6} (**P($F_{49}C_1$-DTBT)**) → $\mu_{h,blend}$ = 9.4 × 10^{-5} cm^2 V^{-1} s^{-1} (**P($F_{49}C_1$-DTBT)**:$PC_{71}BM$), consistent with Blom's results, who reported an example for the more than 2 orders of magnitude increased hole mobility of a blend ($\mu_{h,blend}$), compared to its polymer value ($\mu_{h,polymer}$).[9,17]

The improvements in the FF and J_{SC} of the device might be related to the morphology of the blends. Figure 5 shows atomic force microscopy (AFM) images for a neat **P(2,7F-DTBT)** and a neat **P($F_{45}C_5$-DTBT)**, and transmission electron microscopy (TEM) images for a blend of **P(2,7F-DTBT)**:$PC_{71}BM$ (1:4) and a blend of **P($F_{45}C_5$-DTBT)**:$PC_{71}BM$ (1:4). The neat **P($F_{45}C_5$-DTBT)** film formed more fibril structure than the neat **P(2,7F-DTBT)** film as seen in the AFM images (compare parts a and b of Figure 5), probably leading to the higher μ_h, polymer (2.7 × 10^{-6} vs 4.1 × 10^{-6} cm^2 V^{-1} s^{-1}). TEM images provide a great difference between two blend films of **P(2,7F-DTBT)**:$PC_{71}BM$ and **P($F_{45}C_5$-DTBT)**:$PC_{71}BM$ (compare parts c and d of Figure 5). The domain size for the blend of

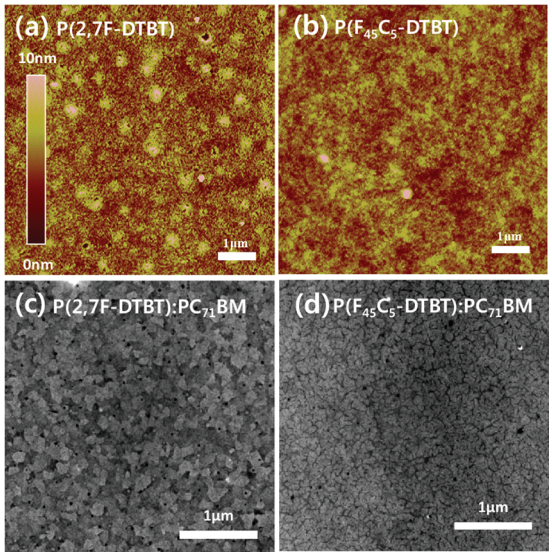

Figure 5. AFM images of neat **P(2,7F-DTBT)** (a), neat **P($F_{45}C_5$-DTBT)** (b). TEM images of a blend of **P(2,7F-DTBT)**:$PC_{71}BM$ (1:4) (c), and a blend of **P($F_{45}C_5$-DTBT)**:$PC_{71}BM$ (1:4) (d).

dx.doi.org/10.1021/ma3002438 | Macromolecules 2012, 45, 3004−3009

P(F$_{45}$C$_5$-DTBT):PC$_{71}$BM is much smaller than that of **P(2,7F-DTBT)**:PC$_{71}$BM. This morphology might be favorable for charge separation and the formation of percolation paths, leading to the improved $\mu_{h,blend}$ and high-efficiency solar cells. Hence, we can speculate that the phase separation can be controlled by the incorporation of 5 mol % 3,6-carbanzole into **P(2,7F-DTBT)**. This led to a good balance between $\mu_{e,blend}$ and $\mu_{h,blend}$ in the device.[12]

In summary, we have demonstrated a novel concept to improve PCE using easily scalable monomers. The incorporation of 3,6-carbazole into **P(2,7F-DTBT)** induced nanoscale morphology of the blends, improving the hole mobility. This result led to a good balance between the electron and hole mobilities in the device (μ_e/μ_h = 152 for **P(2,7F-DTBT)** → μ_e/μ_h = 1.8 for **P(F$_{45}$C$_5$-DTBT)**. The well-balanced mobility almost doubled the PCE (to 5.1%) relative to that of **P(2,7F-DTBT)** (2.6%).

■ ASSOCIATED CONTENT

Ⓢ Supporting Information

J−*V* characteristics for the devices fabricated from various ratios of copolymer PC$_{71}$BM and different annealing temperatures. UV−vis absorption spectra, DSC thermograms, cyclic voltammograms, and the SCLC characteristics of the copolymers. This material is available free of charge via the Internet at http://pubs.acs.org.

■ AUTHOR INFORMATION

Corresponding Author

*E-mail: taihopark@postech.ac.kr.

Author Contributions

†These authors contributed equally.

Notes

The authors declare no competing financial interest.

■ ACKNOWLEDGMENTS

This work was supported by grants from the Energy R&D Program (20093020010040) funded by the MKE, the Basic Science Research Program (No. 2009-0093462), and the Future-based Technology Development Program (Nano Fields, No. 2010-0019119) through the NRF, funded by the MEST (Korea), and by the second stage of a BK21 (Brain Korea 21) grant. Partial support for this work was provided by POSCO.

■ REFERENCES

(1) (a) Chen, J. W.; Cao, Y. *Acc. Chem. Res.* **2009**, *42*, 1709. (b) Gunes, S.; Neugebauer, H.; Sariciftci, N. S. *Chem. Rev.* **2007**, *107*, 1324.

(2) (a) Dennler, G.; Scharber, M. C.; Brabec, C. J. *Adv. Mater.* **2009**, *21*, 1323. (b) Yu, G.; Gao, J.; Hummelen, J. C.; Wudl, F.; Heeger, A. J. *Science* **1995**, *270*, 1789. (c) Rice, A. H.; Giridharagopal, R.; Zheng, S. X.; Ohuchi, F. S.; Ginger, D. S.; Luscombe, C. K. *ACS Nano* **2011**, *5*, 3132.

(3) (a) Chu, T. −Y.; Lu, J.; Beaupré, S.; Zhang, Y.; Pouliot, J. −R. M.; Wakim, S.; Zhou, J.; Leclerc, M.; Li, Z.; Ding, J.; Tao, Y. *J. Am. Chem. Soc.* **2011**, *133*, 4250. (b) Zhou, H.; Yang, L.; Stuart, A. C.; Price, S. C.; Liu, S.; You, W. *Angew. Chem., Int. Ed.* **2011**, *50*, 2995.

(4) (a) Hou, J. H.; Chen, H. Y.; Zhang, S. Q.; Chen, R. I.; Yang, Y.; Wu, Y.; Li, G. *J. Am. Chem. Soc.* **2009**, *131*, 15586. (b) Chen, M. H.; Hou, J.; Hong, Z.; Yang, G.; Sista, S.; Chen, L. M.; Yang, Y. *Adv. Mater.* **2009**, *21*, 4238. (c) Wang, E.; Hou, L.; Wang, Z.; Hellström, S.; Zhang, F.; Inganäs, O.; Andersson, M. R. *Adv. Mater.* **2010**, *22*, 5240.

(5) Chen, H.-Y.; Hou, J.; Zhang, S.; Liang, Y.; Yang, G.; Yang, Y.; Yu, L.; Wu, Y.; Li, G. *Nat. Photonics* **2009**, *3*, 649.

(6) (a) Bernius, M. T.; Inbasekaran, M.; O'Brien, J.; Wu, W. *Adv. Mater.* **2000**, *12*, 1737. (b) Leclerc, M. *J. Polym. Sci., Part A: Polym. Chem.* **2001**, *39*, 2867. (c) Scherf, U.; List, E. J. W. *Adv. Mater.* **2002**, *14*, 477. (d) Cho, S. Y.; Grimsdale, A. C.; Jones, D. J.; Watkins, S. E.; Holmes, A. B. *J. Am. Chem. Soc.* **2007**, *129*, 11910.

(7) (a) Zhang, F.; Kim, G. J.; Bjorström, C.; Scensson, M.; Andersson, M. R.; Sundström, V.; Magnusson, K.; Moons, E.; Yrkady, A.; Inganäs, O. *Adv. Funct. Mater.* **2006**, *16*, 667. (b) Yohannes, T.; Zhang, F.; Scensson, M.; Hummelen, J. C.; Andersson, M. R.; Inganäs, O. *Thin Solid Films* **2004**, *449*, 152.

(8) (a) Berson, S.; Bettignies, R.; Severine, B.; Stephane, G. *Adv. Funct. Mater.* **2007**, *17*, 1377. (b) Kim, J. S.; Lee, J, H.; Park, J. H.; Shim, C.; Sim, M.; Cho, K. *Adv. Funct. Mater.* **2011**, *21*, 480. (c) Deibel, C.; Strobel, T.; Dyakonov, V. *Adv. Mater.* **2010**, *22*, 4097. (d) Chen, S.; Choudhury, K. R.; Subbiah, J.; Amb, C. M.; Reynolds, J. R.; So, F. *Adv. Energy Mater.* **2011**, *1*, 963.

(9) Mihailetchi, V. D.; Xie, H.; de Boer, B.; Koster, L. J. A.; Blom, P.W. M. *Adv. Funct. Mater.* **2004**, *14*, 865.

(10) Kim, J.; Kwon, Y.; Shin, W.; Moon, S.; Park, T. *Macromolecules* **2011**, *44*, 1909.

(11) Fu, Y.; Kim, J.; Siva, A.; Shin, W.; Moon, S.; Park, T. *J. Polym. Sci., Part A: Polym. Chem.* **2011**, *49*, 4368.

(12) Mandoc, M. M.; Koster, L. J. A.; Blom, P. W. M. *Appl. Phys. Lett.* **2007**, *90*, 133504.

(13) Hou, Q.; Xu, Y.; Yang, W.; Yuan, M.; Peng, J.; Cao, Y. *J. Mater. Chem.* **2002**, *12*, 2887.

(14) (a) Park, J. H.; Kim, J. S.; Lee, J. H.; Lee, W. H.; Cho, K. *J. Phys. Chem. C* **2009**, *113*, 17579. (b) Mihailetchi, V. D.; Blom, P. W. M.; Hummelen, J. C.; Rispens, M. T. *J. Appl. Phys.* **2003**, *94*, 6849.

(15) Iraqi, A.; Wataru, I. *J. Polym. Sci., Part A: Polym. Chem.* **2004**, *42*, 6041.

(16) (a) Bijleveld, J. C.; Zoombelt, A. P.; Mathijssen, S. G. J.; Wienk, M. M.; Turbiez, M.; de Leeuw, D. M.; Janssen, R. A. J. *J. Am. Chem. Soc.* **2009**, *131*, 16616. (b) Kumar, A.; Liao, H.-H.; Yang, Y. *Org. Electron.* **2009**, *10*, 1615. (c) Mandoc, M. M.; Koster, L. J. A.; Blom, P. W. M. *Appl. Phys. Lett.* **2007**, *90*, 133504.

(17) Mihailetchi, V. D.; Koster, L. J. A.; Blom, P. W. M.; Melzer, C.; de Boer, B.; van Duren, J. K. J.; Janssen, R. A. J. *Adv. Funct. Mater.* **2005**, *15*, 795.